

Unique determination of ‘sub-atomic’ contrast by imaging covalent backbonding

Adam Sweetman^{*,†} Philipp Rahe^{2,‡} and Philip Moriarty^{1†}

¹*The School of Physics and Astronomy, The University of Nottingham, Nottingham, NG7 2RD, U.K., and* ²*Department of Physics and Astronomy, The University of Utah, Salt Lake City, UT-84112, USA*

E-mail: adam.sweetman@nottingham.ac.uk

Abstract

The origin of so-called ‘sub-atomic’ resolution in dynamic force microscopy (DFM) has remained controversial since its first observation in 2000. A number of detailed experimental and theoretical studies have identified different possible physicochemical mechanisms potentially giving rise to ‘sub-atomic’ contrast. In this study we are able, for the first time, to assign the origin of a specific instance of ‘sub-atomic’ contrast as being due to the back bonding of a surface atom in the tip – sample junction.

Introduction

Since atomic resolution was first obtained by scanning probe microscopy (SPM),¹ scanning tunnelling microscopy (STM) and atomic force microscopy (AFM) have become invaluable tools for both surface science and nanoscience. Despite more than 30 years of striking results, however,

^{*}To whom correspondence should be addressed

^{†1}The School of Physics and Astronomy, The University of Nottingham, Nottingham, NG7 2RD, U.K.

^{‡2}Department of Physics and Astronomy, The University of Utah, Salt Lake City, UT-84112, USA

it is well known that the interpretation of scanning probe images is often complicated due to the variety of tip structures that are observed. In recent years a focus has developed on determining the structure of the very apex of the tip by combining experiment with detailed theoretical calculations²⁻⁴ or by inverse imaging of the tip on a known surface moiety.⁵⁻⁷ A parallel stream of work, pioneered by the group at IBM Zurich, involves the functionalisation of a metal tip with a known molecule or atom in order to provide a well defined termination. This has been key to both obtaining, and interpreting, striking sub-molecular resolution on planar organic molecules in dynamic force microscopy (DFM) - also known as non-contact atomic force microscopy (NC-AFM).⁸

Although Giessibl et al. coined the term "sub-atomic contrast" in 2000⁹ in relation to imaging of the Si(111)-(7x7) surface, their results were critiqued by Hug and co-workers.¹⁰ In Giessibl et al's work,⁹ features in the images of adatoms of the Si(111) surface were assigned to a "double lobe" tip, and interpreted as resulting from a tip with a single terminating silicon atom with two exposed dangling bonds. Soon after publication, it was suggested that the features may have arisen as a result of feedback artefacts, in part based on the observation that the shape of the double lobes changed with reversal of the scan direction.¹⁰ Subsequently, it was shown that these features could be reproduced with the lobes aligned in directions not perpendicular to the scan direction,¹¹ and theoretical calculations suggested that the double lobe features might indeed be observable.¹²

However, it should be noted that due to the computational constraints of the time these simulations involved a number of simplifications, including the use of very small tip-clusters and the fixing of the tips atoms during the calculation of the tip-sample forces. Later, more sophisticated calculations¹³ performed without these limitations suggested that the original model put forward to explain the double lobe features was perhaps over-simplified, and, even if unphysically constrained, did not produce the "double lobe" features observed experimentally or observed in earlier simulations. In addition, other simulations¹⁴ suggested that double lobe features might also arise from complex electron scattering effects, occurring during tunnelling into the surface adatoms at very specific biases from a double lobe terminated tip. The force calculations in this instance, however, assumed a direct proportionality between force and tunnel current, which later experimental

work¹⁵ suggested may not hold for moderately doped semiconductor surfaces. Moreover, Zotti et al.'s calculations suggested that the double lobe structure would be observed only within a specific range of (negative) bias voltages.

Most recently, an even more detailed theoretical study¹⁶ convincingly showed that “double lobe” features with the a similar spacing to that observed experimentally could be produced by tips modelled as dimer-terminated silicon clusters with adsorbed contaminants, providing an alternative explanation for the double lobe features. We note that multi-lobe features within the spatial size of a single atom in the *dissipation* channel have been reported during very close approach,¹⁷ although these clearly have a different origin to the double lobe features discussed above.

In parallel with the debate focused on the silicon – silicon system, further experimental results suggested different symmetric structures could be observed using a graphite surface to probe a tungsten tip,¹⁸ and in this instance the features were assigned to different crystallographic orientations of the tip apex. This work was followed up with a more detailed study where tungsten tips were imaged by single carbon monoxide molecules absorbed on a Cu(111) surface.¹⁹ Again, ‘sub-atomic’ features were observed, and assigned to different multi-pole charges induced on the frontmost tungsten atom due to the different crystallographic orientations. A detailed theoretical study was performed shortly afterwards, which suggested that the same features could be observed in simulation.²⁰ However, it was not possible reach a definitive interpretation of the experimental results, as, depending on the tip orientation, the simulations suggested that ‘sub-atomic’ resolution could occur either as a result of the induced charge density at the tip apex, *or* due to the back bonding of the tip apex.

It is at this juncture necessary to clarify the nomenclature to be used throughout the rest of the paper. It is trivial to show that features can be observed in both STM and AFM that have a spatial resolution smaller than the apparent size of a single atom. In STM a particularly elegant example is the demonstration that information can be encoded with ‘sub-atomic’ spatial resolution in the electronic density of states associated with the electron waves at the surface of a metal crystal.²¹ However although in this instance the features are ‘sub-atomic’ in size, they are not assigned as

having arisen from ‘inside’ a single atom. In regard to DFM, our group recently demonstrated sub-molecular resolution on a tip absorbed C_{60} , which produces what could be termed ‘sub-atomic’ contrast on each adatom of the Si(111) surface⁷ (with feature spacings similar to that reported in the original observation of ‘sub-atomic’ features). But here it is unambiguous that the multiple features within the atoms come not from any ‘sub-atomic’ feature, but rather from the five atoms of the pentagon face of the C_{60} , compressed in size due to the relative flexibility of the tip. Consequently, we wish to make it clear that there is no controversy as to whether features with a smaller spatial size than a single atom can be observed in SPM. The controversy is only in regard as to whether these features truly arise from “inside” a single atom, i.e. as to whether they are truly ‘sub-atomic’ in origin. From this point on we will use the term “sub-atomic like” to refer to features of the first kind (i.e. those features that have a spatial resolution smaller than a single atom, but which arise as a result of multi-atom interaction), and “true sub-atomic” to refer to features that arise from inside a single atom.

In this paper, we unambiguously show that “sub-atomic like” features can arise from the back bonding configuration of a surface atom being imaged during DFM. This is done by utilising the change in bonding configuration of the surface adatoms of the Si(111) unit cell between the faulted and unfaulted half. Due to this change in symmetry across the unit cell, the features we observe cannot be assigned to any tip, or feedback artefacts. At the same time, they suggest caution should be used when interpreting “sub-atomic like” features, as our data cannot be interpreted as arising from within a single atom.

Experimental methods

All experiments in this paper were carried out using an Omicron Nanotechnology LT STM/DFM in the qPlus configuration and carried out in a low temperature cryostat cooled to approximately 78 K using liquid nitrogen, in ultrahigh vacuum (UHV) (base pressure of 5×10^{-11} mbar or better). Clean Si(111) samples were prepared by the standard method of degassing a silicon wafer, flash heating to

1200°C, quickly cooling to 900°C and then slowly cooling to room temperature in order to obtain a good reconstruction. After preparation the silicon sample was transferred directly into the scan head for imaging. We used commercially supplied qPlus sensors from Omicron Nanotechnology, and these were introduced into the UHV chamber and then directly into the scan head without any further preparation.

When we first introduce the sensors and approach the surface, we rarely obtain atomic resolution immediately, most likely due to the oxide layer which forms on electrochemically etched tungsten wires during etching. Consequently, we prepare our tips by standard STM methods, including tip pulsing and controlled crashes into the surface. This is done until good STM resolution is obtained. We then usually select a small area, and transfer to DFM imaging.

Normally, after this form of tip preparation, we obtain “conventional” resolution of the silicon adatoms. This suggests that the tip has a strong chemical interaction with the surface,^{3,4,22} and the adatoms image as circular protrusions in constant frequency shift imaging. However, we very rarely observe “contrast inversion” where the adatoms image as depressions in constant Δf feedback.²³ We note explicitly that we only refer to imaging at 0 V_{gap} or very close to 0 V_{gap} , and hence to a different phenomenon to that reported where contrast inversion occurs due to the so-called “phantom force”¹⁵ induced due to large tunnel currents, or any effect due to electronic crosstalk.²⁴

In addition to imaging, we also present quantitative force data. This was acquired by taking a $\Delta f(z)$ measurement on an adatom, and then a cornerhole of the surface. The cornerhole (off) data is then subtracted from the adatom (on) data in order to produce a “short-range” $\Delta f(z)$. This on versus off method (as used by Lantz et al.²² and Ternes et al.²⁵) removes the non-site-specific long-range forces and produces a $\Delta f(z)$ curve containing only contributions from the short-range forces. This short-range $\Delta f(z)$ was then inverted to force using the Sader-Jarvis algorithm.²⁶ We explicitly note that this method only produces absolute “short-range” forces if the off curve contains no site-specific force contributions. Although the cornerhole is generally considered large enough to fulfil this criterion in DFM experiments, the data in this paper are likely acquired at

much closer approach than conventional (attractive imaging) DFM experiments. Consequently, statements about the size and magnitude of the site-specific force are strictly only relative measurements of the tip-sample force over the adatom versus the tip-sample force over the cornerhole. If there is any residual site-specific contribution over the cornerhole then we would expect the resultant forces to systematically underestimate the true force by a small amount.

Below, we present images taken in both constant Δf feedback, and constant height mode. In constant height mode an attractive interaction is imaged as a decrease in frequency shift, and as such appears as a dark depression in a map of frequency shift. This is the opposite to constant Δf feedback imaging, where an attractive interaction means that the tip will pull back from the surface in order to maintain a constant frequency shift, and as such will image as a bright protrusion. During constant height imaging, a custom-built atom tracking unit²⁷ was used in order to both measure, and then correct thermal drift by applying feedforward correction in between each scan.

Experimental results

In Figure 1 we show results obtained shortly after approaching a clean, freshly prepared, Si(111) sample with a newly introduced sensor. The measurements were conducted immediately after first approach to the clean surface and consequently both tip and surface were as close as possible to their ‘native’ state (i.e. clean silicon, tungsten oxide coated tip).

After a short period of standard STM tip preparation, we obtained good STM resolution, and on transferring to AFM initially observed “conventional” resolution with a slight asymmetry on the adatoms.²⁸ However, during imaging we encountered a surface adsorbate, resulting in a slight tip change. After stopping and restarting the scan we observed a striking change in contrast, shown in Figure 1A. The first feature of note is that the adatoms, and strikingly also the rest atoms, of the surface image as depressions rather than protrusions. The second feature is that the atoms have a very clear triangular symmetry, and that this symmetry changes between the faulted and unfaulted half of the unit cell. We also observe a different form of “sub-atomic like” resolution in

the simultaneously acquired tunnel current signal, with a decrease in the recorded tunnel current at the very centre of the adatoms. However, we note that in this instance we cannot completely discount the effect on the recorded tunnel current due to the topographic feedback, and we do not necessarily assign an unambiguous physical interpretation to the tunnel current data. Importantly, the “sub-atomic like” features in the topography remain present when the gap voltage was reduced to 0V and no tunnel current was recorded (Figure 1C and D).

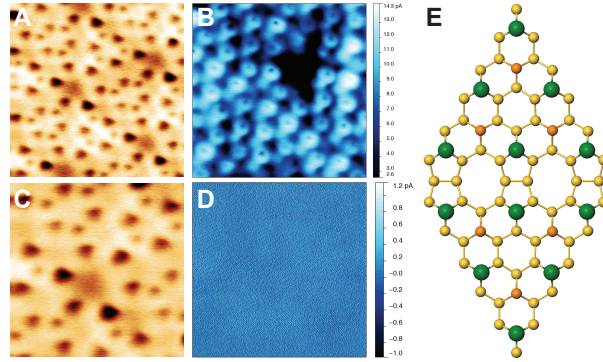


Figure 1: A: constant frequency shift image of the Si(111) 7x7 surface, showing inverted contrast and rest atom resolution, taken with $\Delta f = -10.6$ Hz, oscillation amplitude (A_0) = 275pm, $V_{gap} = +5$ mV. B: simultaneously acquired tunnel current image. C: high-resolution image of the same area taken with $V_{gap} = 0$ mV, D: simultaneously acquired tunnel current image. E: Ball and stick model of the Si(111) 7x7 unit cell with adatoms highlighted in green and rest atoms highlighted in orange.

In order to simplify the interpretation of the imaging, we switched to imaging in constant height mode in the same region. Figure 2 shows a series of images taken at decreasing tip-sample distance, showing the progression in contrast as the tip approaches the surface. Far from the surface we observed no site-specific interaction (Figure 2A), but slightly closer we observed a very weak attractive interaction over the adatoms (Figure 2B). We note here that for “conventional” imaging the adatoms would continue to image as dark circles (i.e. attractive interaction) with increasing intensity for several angstroms. With this tip, however, we notice a completely different type of interaction, as stepping in we immediately see a switch to repulsive contrast (Figure 2C), which becomes more intense as the tip approaches the surface (Figure 2D and F). Importantly, we also observe the exact same triangular shape of the surface atoms, and the same switch in triangular symmetry across the two halves of the unit cell, as was observed in constant Δf feedback. At

very close approach we also observe an attractive feature in the centre of the triangles (Figure 2F), which we will return to below.

By comparing the images shown in both Figure 1 and in Figure 2 with the ball and stick model of the Si(111) unit cell shown in Figure 1E, it is immediately clear that the only surface feature that shares the triangular symmetry of the adatoms is the back bonding configuration of those same atoms. Consequently, we are able to use the switch in the symmetry of the back bonding between the faulted and unfaulted half to unambiguously assign the triangular symmetry to the back bonding configuration. Were the triangular shape to arise from the tip, or any other aspect of the adatoms, then we would not expect to see any change between the faulted and unfaulted half (other than perhaps a change in intensity, rather than a change in symmetry).

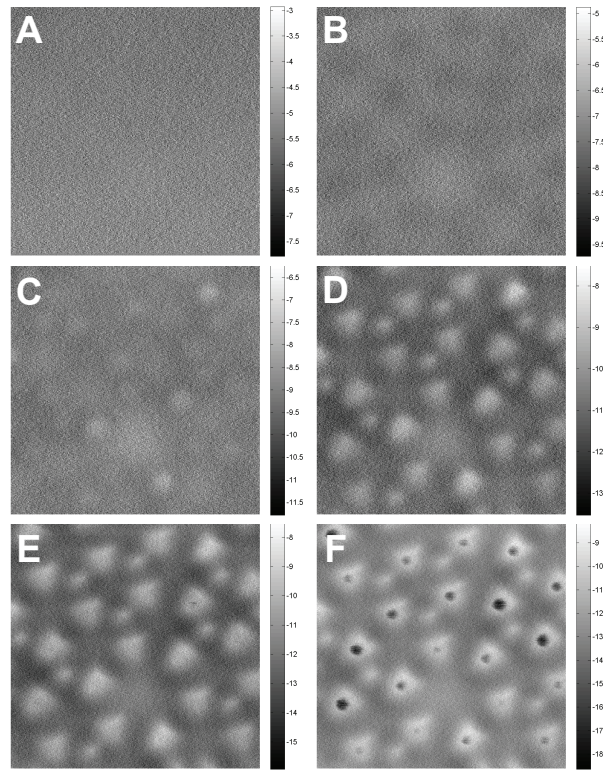


Figure 2: Sequence of constant height images taken with decreasing tip sample height. Oscillation amplitude = 275pm. Z heights are given relative to the atom tracking feedback position of -10.6 Hz. A: Z = +300pm, B: Z = +157pm, C: Z = +90pm, D: Z = +36pm, E: Z = +30pm, F: Z = -80pm.

At this juncture, some attention must be given to explaining the origin of the contrast we observe. Typically only the adatoms of the Si(111) surface are imaged during conventional AFM,

and these are imaged as protrusions in constant frequency shift mode. Consequently, our tip must have radically different properties to those normally used.

We are able to obtain quantitative information about the tip-sample interaction by performing “force spectroscopy” experiments on the adatoms. Figure 3 shows the results of force spectroscopy measurements made on the adatoms as described in the experimental methods. The most important feature to note is the extremely small initial minimum in the attractive force between the tip and the atom, on the order of 10 - 50 pN. This is almost 2 orders of magnitude smaller than typical interactions measured between a silicon cluster and a silicon surface (i.e. approximately 2 nN).^{3,4,22} We assign this very small force as being the result of a passivated tip, similar to those described previously.^{3,29,30} This very small attractive force helps explain the contrast inversion observed in constant Δf feedback by taking into account the total Δf values measured. It must be remembered that in NC-AFM the frequency shift is determined not only by the short-range interaction (as discussed above) but also by the long-range van der Waals and electrostatic interaction. Consequently, by inspection of the Δf curves with respect to the $F(z)$ curve, it is clear that during constant Δf feedback at -10.6Hz, the tip had already entered the repulsive branch of the (site specific) force, and stable feedback with negative frequency shifts was only mediated by the presence of the long-range background. This quantitative analysis of the force also explains the very weak attractive interaction we observed some distance from the surface during constant height imaging, and therefore most likely arises from a highly suppressed chemical interaction, combined with local dispersion interactions.³¹

At close approach we begin to see very strong repulsive behaviour, which explains the repulsive contrast observed in Figure 2E. In addition, at very close approach we also observe a sudden jump in the force, to large attractive values, which corresponds to the large depression feature observed in the centre of the triangles. We suggest that this feature occurs due to a relaxation of the passivating element at the end of the tip, possibly exposing the reactive apex to the underlying surface adatom. We also note that similar (although clearly not identical) features were observed in DFT simulations that formed part of a combined experimental and theoretical study of different

tip structures on a partly passivated Si(111) surface.³

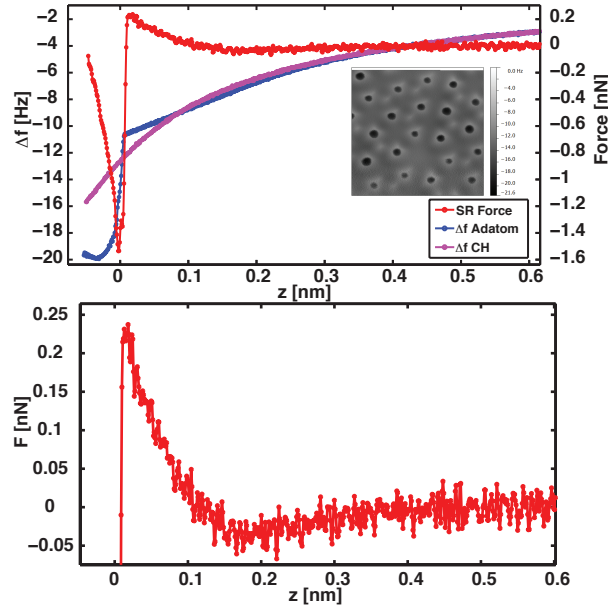


Figure 3: A: Raw $\Delta f(z)$ curves acquired above an adatom, and cornerhole, in the image shown (inset). Also plotted is the site specific $F(z)$. $Z=0$ corresponds to the imaging height. B: Zoom of force curve showing the small attractive well and repulsive regime. From the overlay of the force and Δf we can ascertain that during constant Δf imaging (Figure 1) feedback was occurring in the repulsive part of the short-range force, mediated by the long-range background.

Discussion

Since the symmetry of the surface in this instance allows us to unambiguously assign the “sub-atomic like” contrast on the atoms to the back bonding, it is worth discussing the similarity of our data to other recent results showing ‘sub-atomic’ contrast.

In Welker et. al. and Wright et. al. when the foremost atom is back bonded with a two fold symmetry (W(110) tip) a twofold symmetry is present (both papers); when back bonded with a threefold symmetry (W(111) tip) a threefold symmetry is present (both papers); and back bonded with a four fold symmetry (W(100) tip) results in a circular symmetry experimentally (Welker et al.) or circular/square symmetry in simulation (Wright et al.). In recent results from Hofmann et. al.³² a circular symmetry was observed for both Cu(111) and Cu(100) tips, and a twofold symmetry

for a Cu(110) tip. Consequently we note that an n -fold symmetry in the DFM data does not simply result from n backbonding neighbours. Indeed Wright et al. suggest that the charge density of the tip apex atom may be responsible for ‘sub-atomic’ resolution in some cases, whilst in others it is the back bonding of the tip apex atom that produces the “sub-atomic like” contrast. Intriguingly their simulations suggest that it is the threefold structure that arises from the threefold symmetric backbonding of the tip, a feature with the same symmetry as the “sub-atomic like” contrast in our data.

As noted above, we assign the contrast in our images to a passivated tip. Plausible candidates are tip adsorbed H, OH, or CO, although we note that the same features were not observed with a partially (side adsorbed) CO terminated tip on Si(111) (Fig. 3a of Welker et al.³¹). We also observe a marked increase in the occurrence of this contrast mode after deposition of molecules with passivated end groups,³³ and, consequently, it seems likely that the contrast arises from the passivation of the tip by an unreactive atom or molecule and the resulting suppression of the chemical interaction between the tip and surface.

In the light of our results, it seems plausible that some cases of “sub-atomic like” contrast do arise from variations in the tip-sample force due to the back bonding configuration of the frontmost atom. It is not a trivial to see how these effects can be distinguished from the angular bonding symmetry effects due to induced multi-poles recently claimed to have been observed by Welker et al.,¹⁹ especially if, as has been shown, “sub-atomic like” features can also be observed in the attractive regime due to a flexible ‘multi-apex’ reactive tip.⁷

Conclusions

By the use of a passivated tip on the Si(111) 7x7 surface, we observe “sub-atomic like” contrast on the adatoms. Due to the symmetry of the surface, we are able to unambiguously assign the “sub-atomic like” contrast as arising from the back bonding of the adatoms to the surface, and not to any feature “within” the atom itself, or due to any effect of the tip structure. These results

suggest that more work is required in order to ascertain whether true ‘sub-atomic’ resolution can be unambiguously observed, and interpreted, in DFM. In particular, careful thought must be given to the separation of back bonding and multi-tip effects in the interpretation of ‘sub-atomic’ imaging experiments.

Acknowledgements

P. M. and A. S. thank the Engineering and Physical Sciences Research Council (EPSRC) and the Leverhulme Trust, respectively, for Grants No. EP/G007837/1 and F00/114 BI. P.R. gratefully acknowledges financial support from the Alexander von Humboldt-foundation. The authors would like to acknowledge Samuel Paul Jarvis for numerous stimulating conversations and comments on the manuscript.

Supporting Information Available

Additional experimental results showing the tips state prior to the data presented in the main paper are available as supporting information.

This material is available free of charge via the Internet at <http://pubs.acs.org/>.

References

- (1) Binnig, G.; Rohrer, H.; Gerber, C.; Weibel, E. *Physical review letters* **1983**, *50*, 120–123.
- (2) Sugimoto, Y.; Pou, P.; Custance, O.; Jelinek, P.; Abe, M.; Perez, R.; Morita, S. *Science* **2008**, *322*, 413–417.
- (3) Yurtsever, A.; Sugimoto, Y.; Tanaka, H.; Abe, M.; Morita, S.; Ondráček, M.; Pou, P.; Pérez, R.; Jelínek, P. *Physical Review B* **2013**, *87*, 155403.
- (4) Sugimoto, Y.; Yurtsever, A.; Abe, M.; Morita, S.; Ondráček, M.; Pou, P.; Pérez, R.; Jelínek, P. *ACS Nano* **2013**, *7*, 7370–7376.

- (5) Herz, M.; Giessibl, F.; Mannhart, J. *Physical Review B* **2003**, *68*, 045301.
- (6) Schull, G.; Frederiksen, T.; Arnau, A.; Sánchez-Portal, D.; Berndt, R. *Nature Chemistry* **2010**, *6*, 23–27.
- (7) Chiutu, C.; Sweetman, A. M.; Lakin, A. J.; Stannard, A.; Jarvis, S.; Kantorovich, L.; Dunn, J.; Moriarty, P. *Physical review letters* **2012**, *108*, 268302.
- (8) Gross, L.; Mohn, F.; Moll, N.; Liljeroth, P.; Meyer, G. *Science* **2009**, *325*, 1110–1114.
- (9) Giessibl, F. J.; Hembacher, S.; Bielefeldt, H.; Mannhart, J. *Science* **2000**, *289*, 422–425.
- (10) Hug, H. J.; Lantz, M. A.; Abdurixit, A.; van Schendel, P. J. A.; Hoffmann, R.; Kappenberger, P.; Baratoff, A. *Science* **2001**, *291*, 2509a–2509.
- (11) Giessibl, F. J.; Bielefeldt, H.; Hembacher, S.; Mannhart, J. *Ann. Phys. (Leipzig)* **2001**, *10*, 887–910.
- (12) Huang, M.; Čuma, M.; Liu, F. *Physical review letters* **2003**, *90*, 256101.
- (13) Caciuc, V.; Hölscher, H.; Blügel, S.; Fuchs, H. *Physical review letters* **2006**, *96*, 016101.
- (14) Zotti, L. A.; Hofer, W. A.; Giessibl, F. J. *Chemical Physics Letters* **2006**, *420*, 177–182.
- (15) Weymouth, A.; Wutscher, T.; Welker, J.; Hofmann, T.; Giessibl, F. *Physical review letters* **2011**, *106*.
- (16) Campbellová, A.; Ondráček, M.; Pou, P.; Pérez, R.; Klapetek, P.; Jelínek, P. *Nanotechnology* **2011**, *22*, 295710.
- (17) Sawada, D.; Sugimoto, Y.; Abe, M.; Morita, S. *Applied Physics Express* **2010**, *3*, 116602.
- (18) Hembacher, S.; Giessibl, F. J.; Mannhart, J. *Science* **2004**, *305*, 380–383.
- (19) Welker, J.; Giessibl, F. J. *Science* **2012**, *336*, 444–449.

- (20) Alan Wright, C.; Solares, S. D. *Journal of Physics D: Applied Physics* **2013**, *46*, 155307.
- (21) Moon, C. R.; Mattos, L. S.; Foster, B. K.; Zeltzer, G.; Manoharan, H. C. *Nature Nanotechnology* **2009**, *4*, 167–172.
- (22) Lantz, M. A.; Hug, H. J.; Hoffmann, R.; van Schendel, P. J. A.; Kappenberger, P.; Martin, S.; Baratoff, A.; Güntherodt, H. J. *Science* **2001**, *291*, 2580–2583.
- (23) Sweetman, A.; Jarvis, S.; Danza, R.; Moriarty, P. *Beilstein Journal of Nanotechnology* **2011**, *3*, 25–32.
- (24) Majzik, Z.; Setvín, M.; Bettac, A.; Feltz, A.; Cháb, V.; Jelínek, P. *Beilstein Journal of Nanotechnology* **2012**, *3*, 249–259.
- (25) Ternes, M.; González, C.; Lutz, C. P.; Hapala, P.; Giessibl, F. J.; Jelínek, P.; Heinrich, A. J. *Physical review letters* **2011**, *106*, 016802.
- (26) Sader, J. E.; Jarvis, S. P. *Applied Physics Letters* **2004**, *84*, 1801.
- (27) Rahe, P.; Schutte, J.; Schniederberend, W.; Reichling, M.; Abe, M.; Sugimoto, Y.; Kuhnle, A. *Review of Scientific Instruments* **2011**, *82*, 063704.
- (28) *Additional information can be found in the online supporting information.*
- (29) Sharp, P.; Jarvis, S.; Woolley, R.; Sweetman, A.; Kantorovich, L.; Pakes, C.; Moriarty, P. *Applied Physics Letters* **2012**, *100*, 233120.
- (30) Jarvis, S.; Sweetman, A.; Bamidele, J.; Kantorovich, L.; Moriarty, P. *Physical Review B* **2012**, *85*.
- (31) Welker, J.; Weymouth, A. J.; Giessibl, F. J. *ACS Nano* **2013**, *7*, 7377–7382.
- (32) Hofmann, T.; Pielmeier, F.; Giessibl, F. J. <http://arxiv-web3.library.cornell.edu/abs/1310.6574> **2013**,

- (33) Sweetman, A.; Jarvis, S. P.; Rahe, P.; Champness, N. R.; Kantorovich, L.; Moriarty, P. *Submitted* **2013**,